MATHEMATICAL ENGINEERING
TECHNICAL REPORTS

Laplacian Subdivision and Optimal Schemes

Hiroshi Kawahara da and Kokichi Sugihara

METR 2006–42 July 2006

DEPARTMENT OF MATHEMATICAL INFORMATICS
GRADUATE SCHOOL OF INFORMATION SCIENCE AND TECHNOLOGY
THE UNIVERSITY OF TOKYO
BUNKYO-KU, TOKYO 113-8656, JAPAN

WWW page: http://www.i.u-tokyo.ac.jp/mi/mi-e.htm

Laplacian Subdivision and Optimal Schemes

Hiroshi Kawaharada and Kokichi Sugihara

Department of Mathematical Informatics,
Graduate School of Information Science and Technology,
University of Tokyo

Abstract

This paper proposes new stationary subdivision schemes based on Laplacian smoothing. Moreover, we discuss best choice of elements of stencils.

First, we propose new subdivision schemes with new subdivision matrices which are linear combinations of ordinary subdivision matrices and Laplacian operators. So, we call these schemes "Laplacian subdivision". Laplacian operator can control fairness of surfaces. Similarly, Laplacian subdivisions can control (local) fairness of subdivision surfaces.

Then, we consider Laplacian Loop subdivision and Laplacian butterfly subdivision. Using the analysis in [1,2], we derive a necessary and sufficient condition for Laplacian Loop subdivision to be C^1-continuous. Moreover, we get some C^1 Laplacian butterfly subdivision schemes.

Second, we analyze components of the subdivision schemes. Here, we assume that the subdivision schemes have symmetric stencils and 1-disc subdivision matrix. That is, we consider Loop type subdivision. Then, we can see effects of elements of stencils. Thus, we can get the best choice of elements of stencils. So, we define "optimal scheme" as Loop type subdivision with the best stencil. Optimal schemes generate good subdivision surfaces. On regular part, fairness of some optimal schemes is smaller than that of Loop subdivision.

Key words: Laplacian subdivision, C^1-continuity, Interpolate schemes, Optimal schemes

1 Introduction

Subdivision [3,4] is a well-known method for geometric design and for computer graphics, because the subdivision makes smooth surfaces with arbitrary topology. A subdivision scheme is defined by a rule of change of connectivity and subdivision matrices. Many researchers study the conditions of the continuity of subdivision surfaces depending on the subdivision matrices [4–12].

On the other hand, fairness of surfaces is an important problem for CAGD. Taubin [13] proposed Laplacian based fair surface design. His algorithms require linear time and space complexity. Moreover, he discussed Laplacian smoothing for subdivided meshes. However, he did not discuss the smoothness of limit surfaces of subdivision. The limit surfaces of our Laplacian subdivision are C^1-continuous.

We will derive Laplacian Loop subdivision and Laplacian butterfly subdivision. Our Laplacian subdivision requires linear time and space complexity (Here, we assume the maximal degree of vertices is constant.). In this paper, Laplacian butterfly subdivision is an interpolate subdivision. Our Laplacian butterfly subdivision is C^1-continuous for regular parts. (For extraordinary points, Zorin et al. [14] derived C^1 stencils. However, in this paper, we do not discuss extraordinary points for butterfly subdivision.)

Next, for subdivisions with symmetric stencils and 1-disc subdivision matrix, we analyze components of stencils and discuss (local) fairness and convergence rate of subdivision schemes. Then, we choose the optimal stencil, that is, we can derive optimal subdivision schemes.

2 Ordinary Subdivision

In this section, we review ordinary subdivisions in general.

2.1 Subdivision Matrix

A subdivision scheme is defined by subdivision matrices and a rule of connectivity change. The subdivision scheme, when it is applied to 2-manifold irregular meshes, generates smooth surfaces at the limit. Fig. 1 is an example of the Loop subdivision. In this figure, (a) is an original mesh; subdividing (a), we get (b); subdividing (b) once more, we get (c); subdividing infinite times, we get the smooth surface (d). We call (d) the subdivision surface. Here, a face is divided into four new faces. This is a change of connectivity. In this paper, the change of connectivity is fixed to this type, but other types of connectivity change can be discussed similarly.

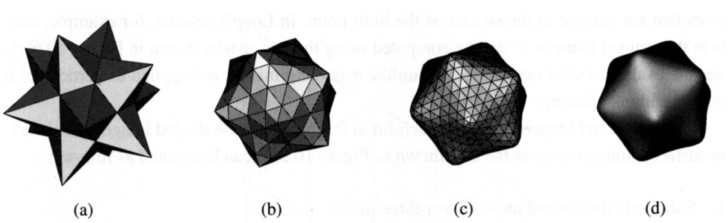

Fig. 1. Loop subdivision [15].

Next, let us consider how to change the positions of the old vertices, and how to decide the positions of the new vertices. They are specified by matrices called "subdivision matrices". The subdivision matrices are defined at vertices and they depend on degree k of the vertex (the degree is the number of edges connected to the vertex). For example, Fig. 2 denotes a vertex v_0^j which has five edges. Let $v_1^j, v_2^j, \cdots, v_5^j$ be the vertices at the other terminals of the five edges. Then, subdivision matrix S_5 is defined as follows:

$$\begin{pmatrix} v_0^{j+1} \\ v_1^{j+1} \\ \vdots \\ v_5^{j+1} \end{pmatrix} = S_5^j \begin{pmatrix} v_0^j \\ v_1^j \\ \vdots \\ v_5^j \end{pmatrix},$$

where v_0^{j+1} is the new locations of the vertex v_0^j after the $j+1$-st subdivision, while $v_1^{j+1}, \cdots, v_5^{j+1}$ are the newly generated vertices.

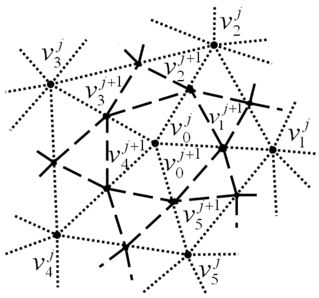

Fig. 2. subdivision matrix.

Here, the subdivision matrix S_5^j is a square matrix. The superscript j means the j-th step of the subdivision. Here, neighbor vertices of a vertex v are called vertices on the 1-disc of v. The subdivision matrix is generally defined not only on vertices in the 1-disc, but also on other vertices around, $\cdots$. Here, we discuss only subdivision matrices that depend on vertices in the 1-disc. However, we can discuss other subdivision matrices, similarly. In this paper, we assume that the subdivision matrix is independent of j. A subdivision scheme of this type is called "stationary".

In this way, the subdivision matrix is written for a vertex. However, since a newly generated vertex is computed by two subdivision matrices at the ends of the edge, the two subdivision matrices must generate the same location of the vertex. So, the subdivision matrices have this kind of restriction.

For example, subdivision matrices S_k $(k \geq 3)$ for the Loop subdivision are

$$S_k = \begin{pmatrix} 1-k\beta & \beta & \beta & \beta & \beta & \beta & \cdots & \beta \\ \frac{3}{8} & \frac{3}{8} & \frac{1}{8} & 0 & 0 & \cdots & 0 & \frac{1}{8} \\ \frac{3}{8} & \frac{1}{8} & \frac{3}{8} & \frac{1}{8} & 0 & 0 & \cdots & 0 \\ \frac{3}{8} & 0 & \frac{1}{8} & \frac{3}{8} & \frac{1}{8} & 0 & \cdots & 0 \\ \vdots & & & & \ddots & & & \\ \frac{3}{8} & \frac{1}{8} & 0 & 0 & \cdots & 0 & \frac{1}{8} & \frac{3}{8} \end{pmatrix},$$

where k is the degree of the associated vertex, and

$$\beta = \frac{1}{k}\left(\frac{5}{8} - \left(\frac{3}{8} + \frac{1}{4}\cos\left(\frac{2\pi}{k}\right)\right)^2\right).$$

The degree k of a vertex is at least two. A vertex whose degree is two is a boundary vertex. The degree of a vertex of 2-manifold meshes is at least three. In this paper, we do not discuss boundaries of meshes. So, we assume that the degree is at least three.

As seen above, a stationary subdivision scheme is defined by subdivision matrices S_k $(k \geq 3)$. Then, by the theorem 2.1 in [8], the limit surface of subdivision f : $|K| \to \mathbf{R}^3$ is the following parametric surface:

$$f[p](y) = \sum_i v_i \phi_i(y),$$
$$v_i \in \mathbf{R}^3,\ \phi_i(y) \in \mathbf{R},\ y \in |K|, p = (v_0, v_1, \cdots),$$

where K is a complex, $|K|$ is a topological space, that is, the mesh, i is an index of a vertex, v_i is the position of the i-th vertex, $p = (v_0, v_1, \cdots)$, and $\phi_i(y)$ is the weight function with the i-th vertex. Moreover, the weight function $\phi_i(y)$ is dependent on the subdivision matrices. If the sum of each row of the subdivision matrix is 1, vertices at each stage of the subdivision is affine combinations of the original vertices. Therefore,

$$\forall y \in |K|,\ \sum_i \phi_i(y) = 1.$$

So, weight functions make affine combinations, too. If the combination is not affine, it is not invariant under the translation of the coordinates systems, and hence we usually consider only affine combinations. Therefore, in what follows we assume that the sum of elements in each row of the subdivision matrix is equal to 1.

Here, we denote $\phi(y) = (\phi_0(y), \phi_1(y), \cdots)$. Then, $\phi(y)$ decides a set of representable surfaces. Then, the set is spanned by $\phi(y)$. So, we call the weight functions basis functions. The limit surface of the subdivision is a point in such a functional space.

3 Laplacian Subdivision

In this section, we define "Laplacian subdivision".

3.1 Laplacian operator

In this paper, we assume that Laplacian operator on meshes is written as:

$$L = I - HA,$$

where I is identity matrix, H is a diagonal matrix, A is the adjacency matrix:

$$H_{ii} = \frac{1}{k_i},\ A_{ij} = \begin{cases} 1 & \text{if vertex } i \text{ is adjacent to vertex } j \\ 0 & \text{otherwise} \end{cases},$$

k_i is the degree of vertex i.

L is diagonalizable, because $HA =$
$H^{1/2}H^{1/2}AH^{1/2}H^{-1/2}$ and $H^{1/2}AH^{1/2}$ is real symmetric matrix. Moreover, from Gershgorin's theorem, we can see that L has real eigen values $2 \geq l_1 \geq l_2 \geq \cdots \geq l_n \geq 0$.

Eigen vectors of L is regarded as natural vibration modes of surfaces, and eigen values of L as natural frequencies.

Here, we can see that $\lim_{j\to\infty} L^j p^0$ is high frequency part of meshes (here, a row of p^0 is a vertex of meshes), and $\lim_{j\to\infty}(L^{-1})^j p^0$ is low frequency part of meshes (here, L^{-1} is a pseudo inverse of L).

3.2 Laplacian subdivision

Here, we assume that subdivision schemes have symmetric stencils. See Fig. 3. Here, $2(b+c) = 1$. For Loop subdivision, $b = \frac{3}{8}, c = \frac{1}{8}, \beta = \frac{1}{k}\left(\frac{5}{8} - \left(\frac{3}{8} + \frac{1}{4}\cos\left(\frac{2\pi}{k}\right)\right)^2\right)$.

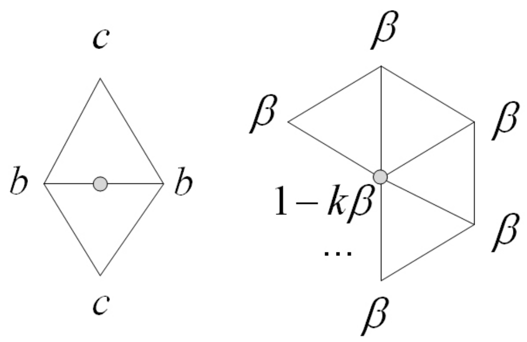

Fig. 3. 1-disc stencils.

Here, we consider the stencil of Laplacian. See Fig. 4. k is degree of the center vertex. So, the sum of elements of this stencil is zero.

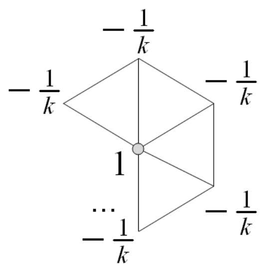

Fig. 4. Stencil of Laplacian.

Now, subdivision matrix of Loop subdivision is:

$$S_k = \begin{pmatrix} 1-k\beta & \beta & \beta & \beta & \beta & \beta & \cdots & \beta \\ \frac{3}{8} & \frac{3}{8} & \frac{1}{8} & 0 & 0 & \cdots & 0 & \frac{1}{8} \\ \frac{3}{8} & \frac{1}{8} & \frac{3}{8} & \frac{1}{8} & 0 & 0 & \cdots & 0 \\ \frac{3}{8} & 0 & \frac{1}{8} & \frac{3}{8} & \frac{1}{8} & 0 & \cdots & 0 \\ \vdots & & & & \ddots & & & \\ \frac{3}{8} & \frac{1}{8} & 0 & 0 & \cdots & 0 & \frac{1}{8} & \frac{3}{8} \end{pmatrix}.$$

Here, we define Laplacian Loop subdivision as subdivision with subdivision matrix S_k^H:

$$S_k^H = S_k + a \begin{pmatrix} 1 & -\frac{1}{k} & \cdots & -\frac{1}{k} \\ 0 & 0 & \cdots & 0 \\ \vdots & \vdots & \vdots & \vdots \end{pmatrix},$$

where $a \in \mathbf{R}$.

So, if $a > 0$, then the limit surface of Laplacian Loop subdivision has more high frequency part. This is high pass Laplacian Loop subdivision.

Next, we consider low pass Laplacian Loop subdivision. Here, we define pseudo inverse of L (L does not have an inverse. Because, L has eigen value 0.). In general, there is a well-known pseudo inverse of L. Let $L = U^{-1}TU, T = \mathbf{diag}(l_1, l_2, \cdots, l_n)$. Then, pseudo inverse $\grave{L}^{-1} = U^{-1}\grave{T}U$, where

$$\grave{T}_{ii} = \begin{cases} \frac{1}{l_i} & \text{if } l_i \neq 0 \\ 0 & \text{if } l_i = 0 \end{cases} .$$

However, the computation of $\grave{L}^{-1}$ requires quadratic time complexity. An important merit of subdivision schemes is thier linear time complexity. So, we do not use $\grave{L}^{-1}$.

As we have seen, $2 \geq l_1 \geq l_2 \geq \cdots \geq l_n \geq 0$. So, we define a pseudo inverse of L as $\acute{L}^{-1} = I - \frac{1}{2}L$. $\acute{L}^{-1} = U^{-1}\acute{T}U$, where $\acute{T} = \mathbf{diag}(1 - \frac{1}{2}l_1, 1 - \frac{1}{2}l_2, \cdots, 1 - \frac{1}{2}l_n)$.

Here, $1 \geq 1 - \frac{1}{2}l_n \geq 1 - \frac{1}{2}l_{n-1} \geq \cdots \geq 1 - \frac{1}{2}l_1 \geq 0$. So, $\lim_{j\to\infty}(\acute{L}^{-1})^j p^0$ is low frequency part.

Here, we can consider stencil of $\acute{L}^{-1}$. See Fig. 5. The sum of elements of this stencil is 1.

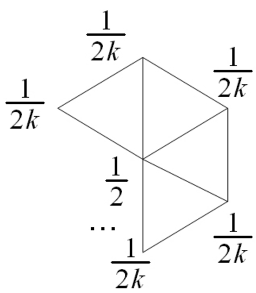

Fig. 5. Stencil of pseudo inverse of Laplacian.

Thus, we define low pass Laplacian Loop subdivision as subdivision with subdivision matrix S_k^L:

$$S_k^L = (1-\acute{a})S_k + \acute{a}\begin{pmatrix} \frac{1}{2} & \frac{1}{2k} & \frac{1}{2k} & \frac{1}{2k} & \frac{1}{2k} & \frac{1}{2k} & \cdots & \frac{1}{2k} \\ \frac{3}{8} & \frac{3}{8} & \frac{1}{8} & 0 & 0 & \cdots & 0 & \frac{1}{8} \\ \frac{3}{8} & \frac{1}{8} & \frac{3}{8} & \frac{1}{8} & 0 & 0 & \cdots & 0 \\ \frac{3}{8} & 0 & \frac{1}{8} & \frac{3}{8} & \frac{1}{8} & 0 & \cdots & 0 \\ \vdots & & & & \ddots & & & \\ \frac{3}{8} & \frac{1}{8} & 0 & 0 & \cdots & 0 & \frac{1}{8} & \frac{3}{8} \end{pmatrix},$$

where $0 \le \acute{a} \le 1$.

So, the limit surface of low pass Laplacian Loop subdivision has more low frequency part.

Note that $\acute{L}^{-1}$ has local stencil. So, $\acute{L}^{-1}$ acts local fairness. On the other hand, $\grave{L}^{-1}$ acts global fairness. That is, $\grave{L}^{-1}$ does not have local (symmetric) stencil. So, $\grave{L}^{-1}$ requires quadratic time complexity. Therefore, the limit surface of low pass Laplacian subdivision has only local low frequency part.

3.3 C^1-continuity of Laplacian subdivision

Here, we consider C^1-continuity of Laplacian Loop subdivision. In [2,16], we derived a necessary and sufficient condition for stationary subdivision schemes to be C^1-continuous. Using the condition, we decide domain a for Laplacian Loop subdivision to be C^1-continuous.

First we consider high pass Laplacian Loop subdivision. Now, $p^{j+1} = S_k^H p^0$. Let

$$\Delta = \begin{pmatrix} 1 & 0 & \cdots & & & \\ -1 & 1 & 0 & \cdots & & \\ -1 & 0 & 1 & 0 & \cdots & \\ \vdots & & & \ddots & & \end{pmatrix}.$$

Using a matrix $\acute{D}_k^H = \Delta S_k^H \Delta^{-1}$, we get

$$\begin{pmatrix} v_0^{j+1} \\ v_1^{j+1} - v_0^{j+1} \\ \vdots \\ v_k^{j+1} - v_0^{j+1} \end{pmatrix} = \acute{D}_k^H \begin{pmatrix} v_0^j \\ v_1^j - v_0^j \\ \vdots \\ v_k^j - v_0^j \end{pmatrix}.$$

Here, we denote the vector consisting of the elements $v_1^j - v_0^j, v_2^j - v_0^j, \cdots, v_k^j - v_0^j$ as d^j and the associated submatrix of $\acute{D}_k^H$ as D_k^H:

$$\acute{D}_k^H = \left(\begin{array}{c|c} * & \acute{*} \\ \hline 0 & \\ \vdots & D_k^H \\ 0 & \end{array}\right).$$

So, $d^{j+1} = D_k^H d^j$. Thus, $D_k^H = D_k + a\frac{1}{k}B$, where $B = \begin{pmatrix} 1 & \cdots & 1 \\ \vdots & \vdots & \vdots \end{pmatrix}$, D_k is such submatrix of Loop subdivision.

$$D_k = \begin{pmatrix} \frac{3}{8} & \frac{1}{8} & 0 & 0 & \cdots & 0 & \frac{1}{8} \\ \frac{1}{8} & \frac{3}{8} & \frac{1}{8} & 0 & 0 & \cdots & 0 \\ 0 & \frac{1}{8} & \frac{3}{8} & \frac{1}{8} & 0 & \cdots & 0 \\ & & & \ddots & & & \\ \frac{1}{8} & 0 & 0 & \cdots & 0 & \frac{1}{8} & \frac{3}{8} \end{pmatrix} - \beta B.$$

Now, by discrete Fourier transform, first term of D_k is diagonalizable. Moreover, eigen values of B are $k, 0, 0, \cdots, 0$. Eigen vector of eigen value k is $(1, 1, \cdots, 1)^\top$. Eigen value of eigen vector $(1, 1, \cdots, 1)^\top$ in first term is $\frac{5}{8}$. So, operator B affects only this eigen space of first term.

Thus, D_k and D_k^H are diagonalizable, too. Eigen values of D_k^H are $\frac{5}{8} - k\beta + a, \frac{3}{8} + \frac{2}{8}\cos(\frac{2\pi}{k}), \frac{3}{8} + \frac{2}{8}\cos(\frac{4\pi}{k}), \cdots, \frac{3}{8} + \frac{2}{8}\cos(\frac{2(k-1)\pi}{k})$.

Therefore, the limit surface of high pass Laplacian Loop subdivision is tangent plane continuous if and only if $\forall k \geq 3, |\frac{5}{8} - k\beta + a| < |\frac{3}{8} + \frac{2}{8}\cos(\frac{2\pi}{k})|$. So, $0 < a < k\beta - \frac{2}{8} + \frac{2}{8}\cos(\frac{2\pi}{k})$.

Here, Loop subdivision is C^1-continuous. Eigen values $\frac{3}{8}+\frac{2}{8}\cos(\frac{2\pi}{k}), \frac{3}{8}+\frac{2}{8}\cos(\frac{2\pi}{k})$ are dominant eigen values. So, B does not affect dominant eigen spaces. Thus, difference vectors of high pass Laplacian Loop subdivision are equal to that of Loop subdivision at the limit. Therefore, if the limit surface of high pass Laplacian Loop subdivision is tangent plane continuous, the limit surface is C^1-continuous.

Next, we consider low pass Laplacian Loop subdivision. Similarly, using a matrix $\acute{D}_k^L = \Delta S_k^L \Delta^{-1}$, we get

$$\begin{pmatrix} v_0^{j+1} \\ v_1^{j+1} - v_0^{j+1} \\ \vdots \\ v_k^{j+1} - v_0^{j+1} \end{pmatrix} = \acute{D}_k^L \begin{pmatrix} v_0^{j} \\ v_1^{j} - v_0^{j} \\ \vdots \\ v_k^{j} - v_0^{j} \end{pmatrix}.$$

Here, we denote submatrix of $\acute{D}_k^L$ as D_k^L:

$$\acute{D}_k^L = \left(\begin{array}{c|c} * & \acute{*} \\ \hline 0 & \\ \vdots & D_k^L \\ 0 & \end{array}\right).$$

Thus, $D_k^L = D_k + \acute{a}(\beta - \frac{1}{2k})B$.

Here, we can see that if $a = \acute{a}(k\beta - \frac{1}{2})$, then high pass scheme is equivalent to low pass scheme. So, if $\forall k \geq 3, |\frac{5}{8} - k\beta + \acute{a}(k\beta - \frac{1}{2})| < |\frac{3}{8} + \frac{2}{8}\cos(\frac{2\pi}{k})|$, then the limit surface of low pass Laplacian subdivision is tangent plane continuous and C^1-continuous.

Note that if $k \geq 4, k\beta - \frac{1}{2} < 0$. However, if $k = 3, k\beta - \frac{1}{2} > 0$. So, since $0 \leq \acute{a} \leq 1$, if $k = 3, a > 0$. That is, low pass Laplacian Loop subdivision at vertex with degree-3 is high pass Laplacian Loop subdivision.

3.4 Examples

In this subsection, we show some examples. Fig. 6 is a torus. Fig. 7 is Loop subdivision surface of the torus. Fig. 8 and Fig. 9 are high pass and low pass Laplacian Loop subdivision surfaces of the torus. Here, $a = k\beta - \frac{2}{8} + \frac{2}{8}\cos(\frac{3\pi}{k}), \acute{a} = 1$.

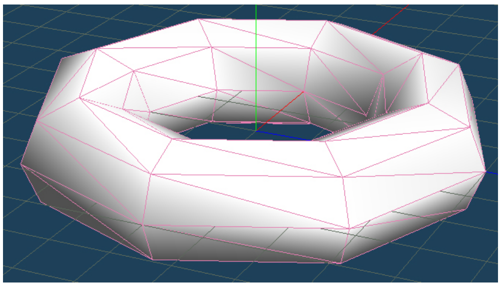

Fig. 6. Torus.

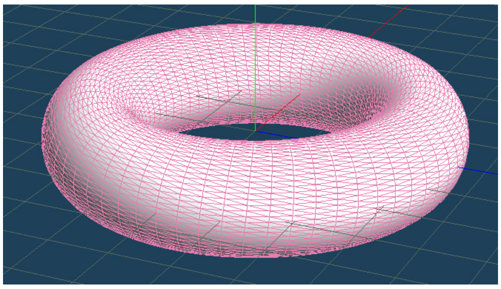

Fig. 7. Loop subdivision surface.

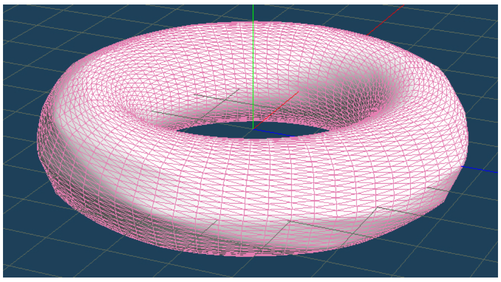

Fig. 8. High pass Laplacian Loop subdivision surface.

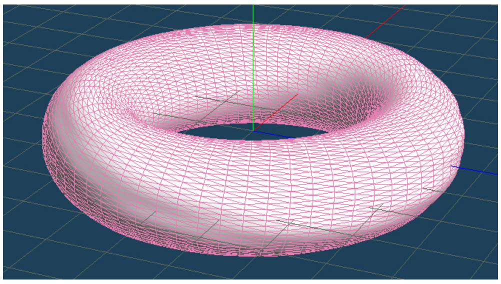

Fig. 9. Low pass Laplacian Loop subdivision surface.

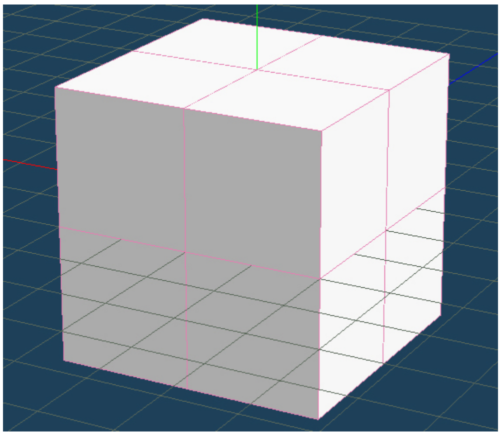

Fig. 10. Cube.

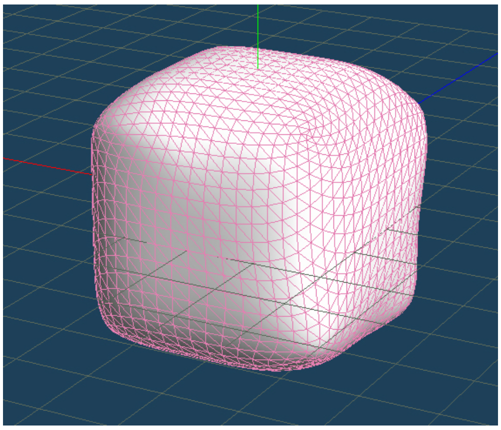

Fig. 11. Loop subdivision surface.

Similarly, Fig. 10 is a cube. Fig. 11 and Fig. 12 and Fig. 13 are Loop and high pass and low pass Laplacian Loop subdivision surfaces of the cube. Here, $a = k\beta - \frac{2}{8} + \frac{2}{8}\cos(\frac{3\pi}{k}), \acute{a} = 1$.

High pass Laplacian Loop subdivision surfaces keep outlines of shapes more than ordinary Loop subdivision surfaces.

The low pass Laplacian Loop subdivision shrinks the limit surface than the limit surface of ordinary Loop subdivision. See Fig. 14 and Fig. 15. The green surfaces are the limit surfaces of Loop subdivision. The pink surfaces are the limit surfaces of low pass Laplacian Loop subdivision.

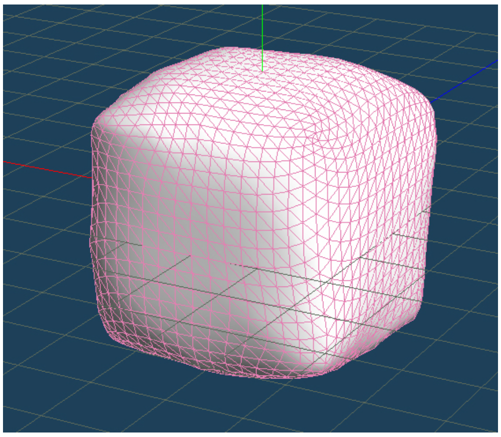

Fig. 12. High pass Laplacian Loop subdivision surface.

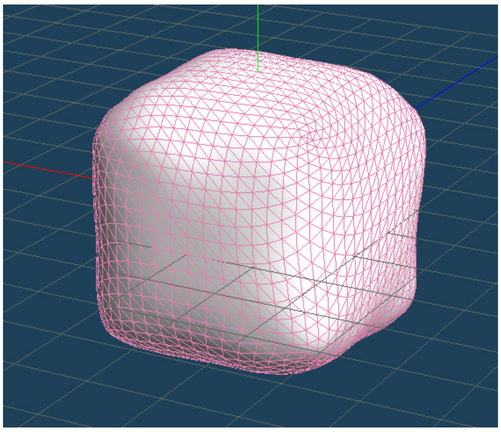

Fig. 13. Low pass Laplacian Loop subdivision surface.

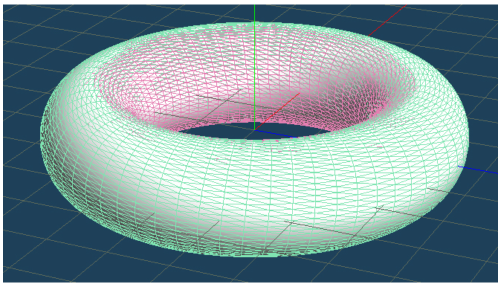

Fig. 14. Loop subdivision and low pass Laplacian Loop subdivision surfaces of torus.

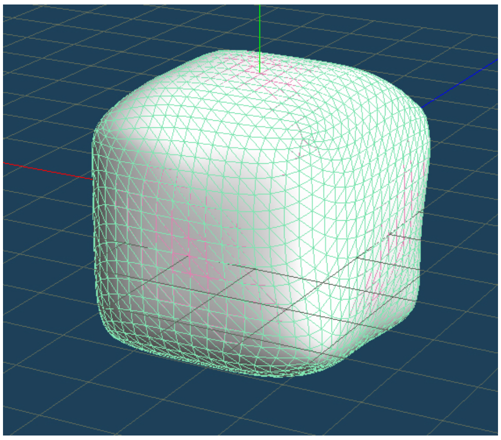

Fig. 15. Loop subdivision and low pass Laplacian Loop subdivision surfaces of cube.

Here, we can see that for the torus, fairness of Loop subdivision surfaces is smaller than that of low pass Laplacian Loop subdivision. Low pass Laplacian Loop subdivision has only local low frequency part. So, global fairness of low pass Laplacian Loop subdivision surfaces is not necessary smaller than that of ordinary Loop subdivision surfaces.

4 Laplacian Butterfly Subdivision

In this section, we consider Laplacian butterfly subdivision. Laplacian butterfly subdivision is an interpolate subdivision scheme. Ordinary butterfly subdivision basis has fairness. In this section, we consider only low pass Laplacian butterfly subdivision. Similarly, we can consider high pass Laplacian butterfly subdivision.

4.1 Low pass Laplacian butterfly subdivision

As in the case of Laplacian Loop subdivision, we consider linear combination of butterfly subdivision matrix and Laplacian operator. However, Laplacian operator affects the position of vertex v_0^0 of original mesh. So, we can not make interpolate Laplacian subdivision.

Therefore, we consider a new operator $\bar{L}$. $\bar{L}$ affects only new generated vertices. See Fig. 16. The left figure is the effect of L with $a < 0$. The right figure is the effect of $\bar{L}$.

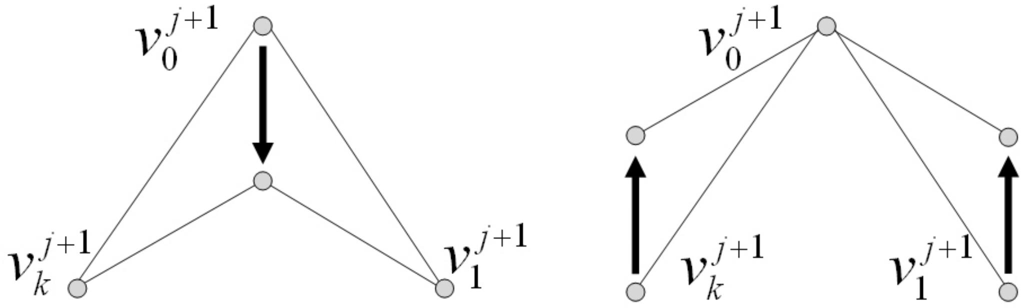

Fig. 16. Laplacian operator for interpolate schemes.

Thus, we define the stencil of $\bar{L}$. Fig. 17 is the stencil of butterfly subdivision (Here, w in [14] is zero.). Fig. 18 is stencil of $\bar{L}$ (See Fig. 5 with $k = 6$.). However, this stencil is not symmetric. So, we consider symmetric stencil. Fig. 19 is symmetric stencil of $\bar{L}$. Thus, we use this stencil.

Then, we can consider low pass Laplacian butterfly subdivision. The stencil of low pass Laplacian butterfly subdivision is convex combination of ordinary butterfly subdivision stencil and symmetric stencil of $\bar{L}$. Here, we denote coefficients of the convex combination as $(1-b), b$, where $0 \leq b \leq 1$. For example, if $b = \frac{1}{4}$, then the stencil of low pass Laplacian butterfly subdivision is the stencil in Fig. 20. However, the interpolate subdivision with this stencil is not C^1-continuous.

Now, we consider C^1-continuity of low pass Laplacian butterfly subdivision. Using our analysis in [2,16], we checked C^1-continuity of $b = \frac{1}{8}$ or $\frac{3}{16}$ (Maybe, $0 \leq b < \frac{1}{4}$, then low pass Laplacian butterfly subdivision is C^1-continuous.). Fig. 21 is the stencil of $b = \frac{1}{8}$. Fig. 22 is the stencil of $b = \frac{3}{16}$.

4.2 Examples

Here, we show some examples of low pass Laplacian butterfly subdivision. Fig. 23 is an original mesh. All degree of vertices of this original mesh is 6. The center

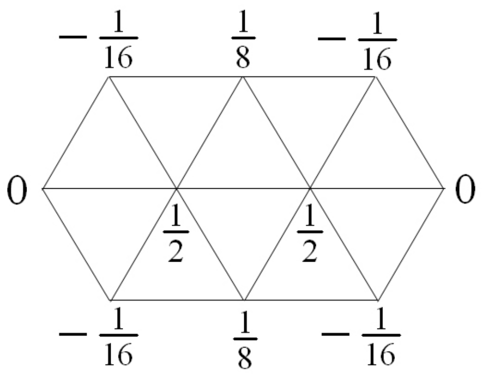

Fig. 17. The stencil of butterfly subdivision.

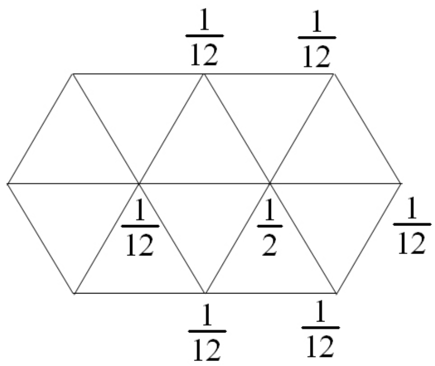

Fig. 18. Non-symmetric stencil of $\bar{L}$.

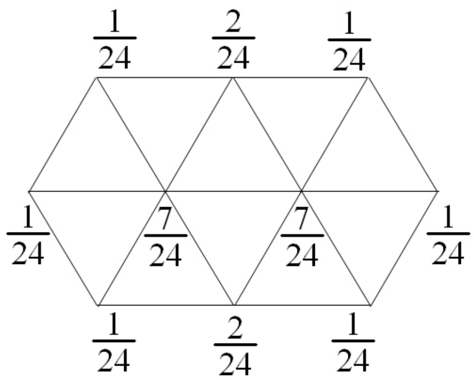

Fig. 19. Symmetric stencil of $\bar{L}$.

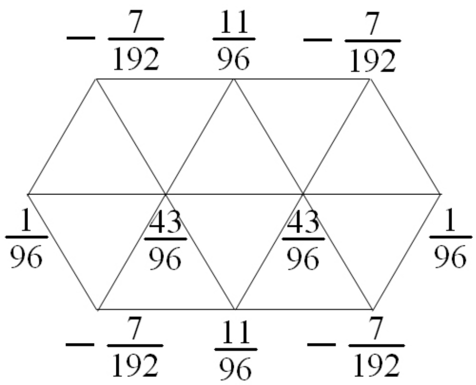

Fig. 20. Non-smooth low pass Laplacian butterfly subdivision stencil.

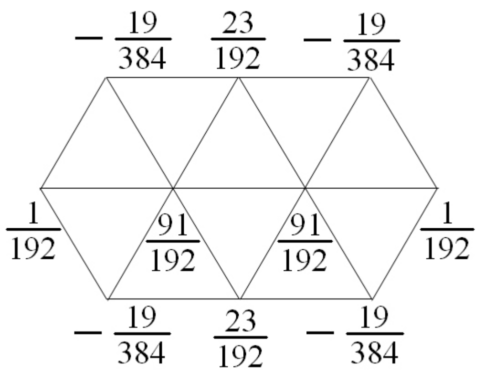

Fig. 21. The stencil of $b = \frac{1}{8}$.

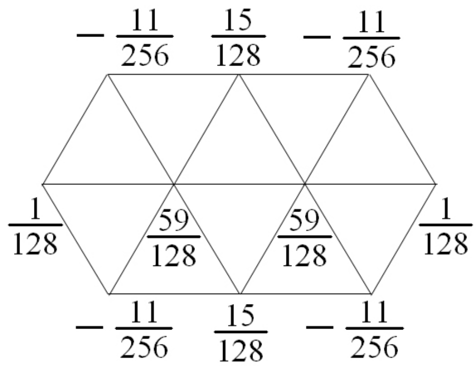

Fig. 22. The stencil of $b = \frac{3}{16}$.

vertex of original mesh is $(0, 0, 1)$. Other vertices of original mesh is on the plane $z = 0$. So, butterfly subdivision surface of this original mesh represents basis function of regular part. Fig. 24 is the butterfly subdivision surface of the original mesh. Fig. 25 is the low pass Laplacian butterfly subdivision with $b = \frac{1}{8}$ of the original mesh. Fig. 26 is that of $b = \frac{3}{16}$.

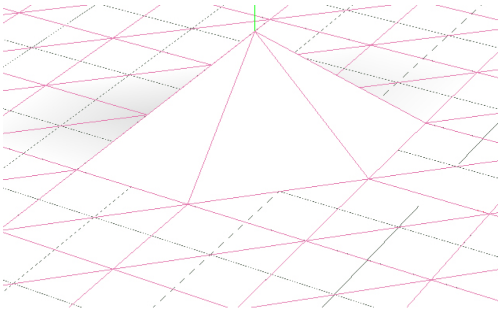

Fig. 23. Original mesh.

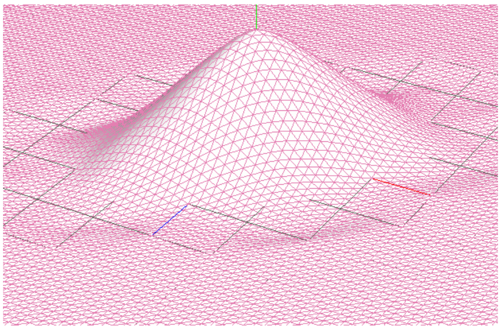

Fig. 24. Basis function of butterfly subdivision.

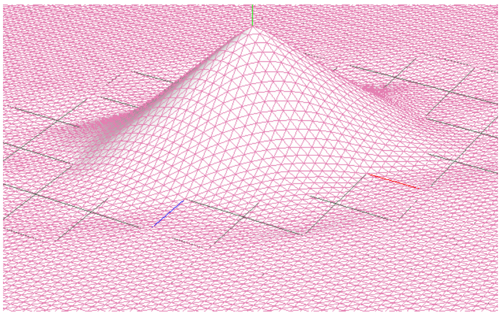

Fig. 25. Basis function of low pass Laplacian butterfly subdivision with $b = \frac{1}{8}$.

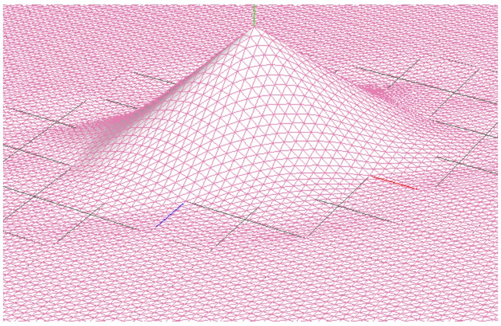

Fig. 26. Basis function of low pass Laplacian butterfly subdivision with $b = \frac{3}{16}$.

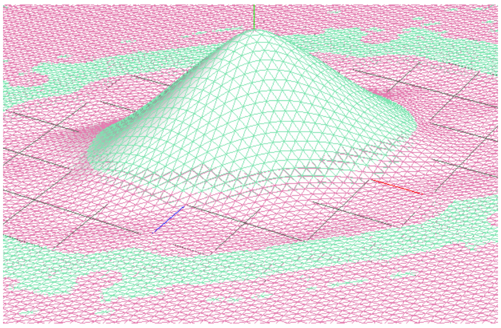

Fig. 27. Basis functions of ordinary butterfly and $b = \frac{1}{8}$.

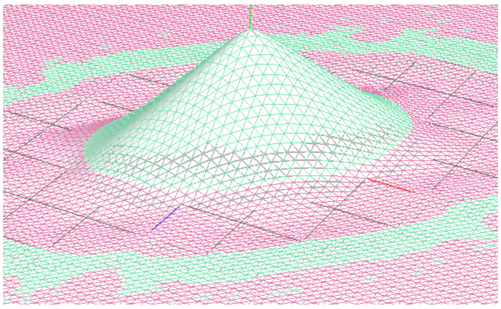

Fig. 28. Basis functions of low pass Laplacian butterfly subdivision with $b = \frac{1}{8}$ and $\frac{3}{16}$.

Fairness of basis functions of $b = \frac{1}{8}$ or $\frac{3}{16}$ is smaller than that of basis function of ordinary butterfly subdivision. In Fig. 27, the green surface is basis function of ordinary butterfly subdivision. The pink surface is basis function of low pass Laplacian butterfly subdivision with $b = \frac{1}{8}$. In Fig. 28, the green surface is basis function of low pass Laplacian butterfly subdivision with $b = \frac{1}{8}$. The pink surface is that with $b = \frac{3}{16}$.

Next, Fig. 29 is a cube. Fig. 30 is the butterfly subdivision surface of the cube. Fig. 31 is the low pass Laplacian butterfly subdivision surface with $b = \frac{1}{8}$ of the cube. Fig. 32 is that of $b = \frac{3}{16}$. Here, we use the stencil in [14] as stencil of extraordinary

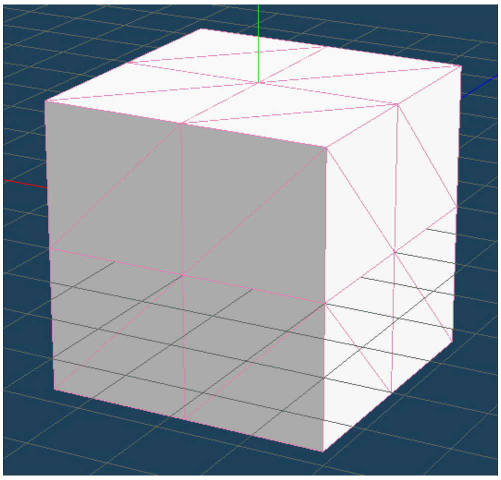

Fig. 29. Original cube.

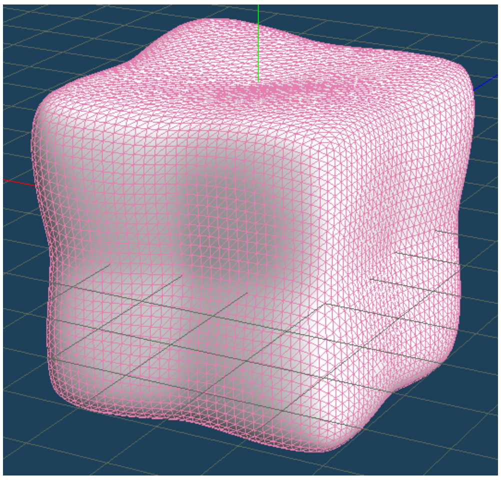

Fig. 30. Butterfly subdivision surface of the cube.

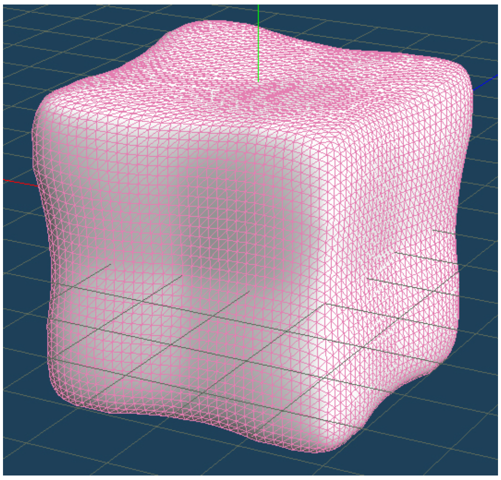

Fig. 31. Low pass Laplacian butterfly subdivision surface with $b = \frac{1}{8}$.

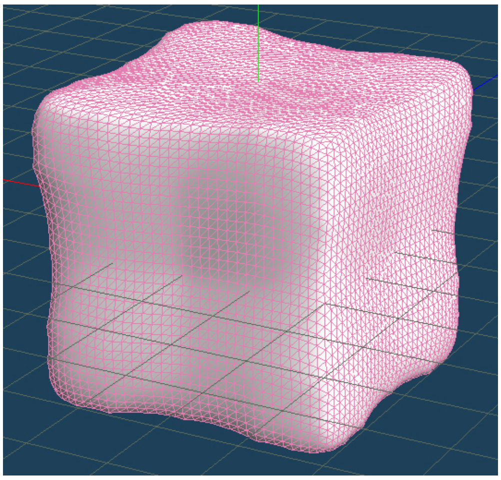

Fig. 32. Low pass Laplacian butterfly subdivision surface with $b = \frac{3}{16}$.

points.

In Fig. 33, the green surface is ordinary butterfly subdivision surface of the cube. The pink surface is low pass Laplacian butterfly subdivision surface with $b = \frac{1}{8}$ of the cube. In Fig. 34, the green surface is low pass Laplacian butterfly subdivision surface with $b = \frac{1}{8}$. The pink surface is that with $b = \frac{3}{16}$.

For this cube, we can not see concrete decrease of fairness between ordinary butterfly subdivision surface and low pass Laplacian butterfly subdivision surfaces with $b = \frac{1}{8}$ and $\frac{3}{16}$. Thus, in the future work, we must discuss stencil of extraordinary points.

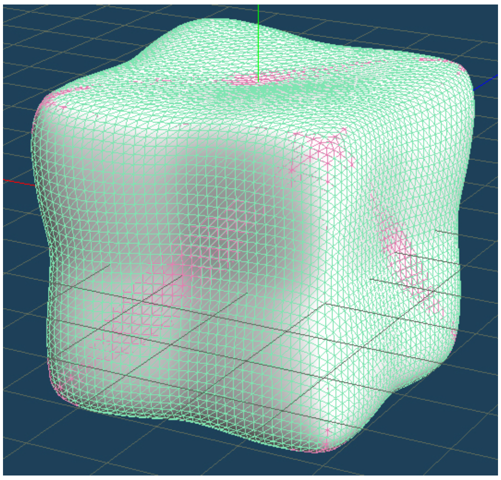

Fig. 33. Low pass Laplacian butterfly subdivision surfaces with $b = 0$ and $\frac{1}{8}$.

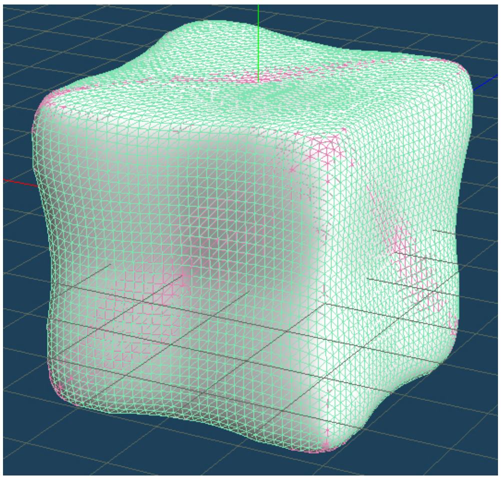

Fig. 34. Low pass Laplacian butterfly subdivision surfaces with $b = \frac{1}{8}$ and $\frac{3}{16}$.

5 Optimal Schemes

In this section, we consider subdivisions with symmetric stencil and 1-disc subdivision matrix. That is, we consider Loop type subdivisions.

In previous section, we see that eigen value $\frac{5}{8} - k\beta$ decides the effect of Laplacian operator. So, next, we consider effects of other eigen values. In fact, other eigen values of D_k affect waves on concentric circles whose center is v_0^j. Eigen value of Laplacian of D_k affects a wave which is vertically on other waves. Thus, we will change elements $\frac{3}{8}, \frac{1}{8}$ of stencil such that the waves on concentric circles are decreased faster. Then, we call a subdivision scheme which has best choice of elements of stencil “optimal scheme”.

5.1 Analysis of Loop type subdivision

Now, we consider Loop type subdivision matrix S_k:

$$S_k = \begin{pmatrix} 1-k\beta & \beta & \beta & \beta & \beta & \beta & \cdots & \beta \\ b & b & c & 0 & 0 & \cdots & 0 & c \\ b & c & b & c & 0 & 0 & \cdots & 0 \\ b & 0 & c & b & c & 0 & \cdots & 0 \\ \vdots & & & & \ddots & & & \\ b & c & 0 & 0 & \cdots & 0 & c & b \end{pmatrix}.$$

For Loop subdivision, $b = \frac{3}{8}, c = \frac{1}{8}, \beta = \frac{1}{k}\left(\frac{5}{8} - \left(\frac{3}{8} + \frac{1}{4}\cos\left(\frac{2\pi}{k}\right)\right)^2\right)$. Then,

$$D_k = \begin{pmatrix} b & c & 0 & 0 & \cdots & 0 & c \\ c & b & c & 0 & 0 & \cdots & 0 \\ 0 & c & b & c & 0 & \cdots & 0 \\ & & & \ddots & & & \\ c & 0 & 0 & \cdots & 0 & c & b \end{pmatrix} - \beta B.$$

Here, we denote the first term of D_k as A. A is diagonalizable by discrete Fourier transform: $A = W^{-1}\Lambda W$. Here, $\Lambda = \mathbf{diag}(b + 2c\cos(\frac{0}{k}), b + 2c\cos(\frac{2\pi}{k}), b + 2c\cos(\frac{2(2)\pi}{k}), b + 2c\cos(\frac{2(3)\pi}{k}), \cdots, b + 2c\cos(\frac{2(k-1)\pi}{k}))$.

$$W = \begin{pmatrix} \omega^0 & \omega^0 & \omega^0 & \cdots & \omega^0 \\ \omega^0 & \omega^1 & \omega^2 & \cdots & \omega^{(k-1)} \\ \omega^0 & \omega^2 & \omega^4 & \cdots & \omega^{2(k-1)} \\ \vdots & \vdots & \vdots & \ddots & \vdots \\ \omega^0 & \omega^{(k-1)} & \omega^{2(k-1)} & \cdots & \omega^{(k-1)^2} \end{pmatrix},$$

where $\omega = e^{-i\frac{2\pi}{k}} = \cos(\frac{2\pi}{k}) - i\sin(\frac{2\pi}{k})$.

Now, the eigen value $b+2c$ of A is eigen value of Laplacian. Other eigen values of A is coefficients of decreases of discrete Fourier transform of difference vectors. Each eigen space of the other eigen values of A represents vibration modes of difference vectors.

Here, in order to be tangent plane continuous, $|b+2c-k\beta| < |b+2c\cos(\frac{2\pi}{k})|$. See Fig. 35. Red points are eigen values of D_k. The center of the circle is $(b, 0)$. The radius of the circle is $|2c|$.

So, if $c > 0, b - 2c \geq 0$, then dominant eigen values of D_k are $b + 2c\cos(\frac{2\pi}{k}), b + 2c\cos(\frac{2(k-1)\pi}{k})$. These eigen values correspond to lowest frequency part of difference vectors. Therefore, D_k^∞ is low pass filter of difference vectors. On the other hand, eigen values $b + 2c\cos(\frac{2\lceil\frac{k}{2}\rceil\pi}{k}), b + 2c\cos(\frac{2\lfloor\frac{k}{2}\rfloor\pi}{k})$ correspond to highest frequency part. These eigen values are smallest eigen values of A. So, components of these eigen spaces decrease fastest.

In fact, If $c > 0, b - 2c \geq 0$, then $D_k^\infty = W^{-1}FW$, where $F = \mathbf{diag}(0, (b +$

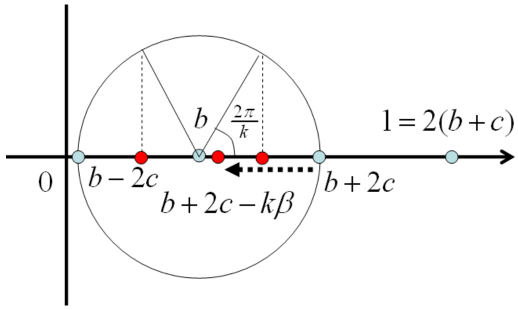

Fig. 35. Eigen values of D_k.

$2c\cos(\frac{2\pi}{k}))^\infty, 0, 0, \cdots, 0, 0, (b + 2c\cos(\frac{2(k-1)\pi}{k}))^\infty)$. Let w_2 be second row of W and w_k be k-th row of W and w_2^{-1} be second column of W^{-1} and w_k^{-1} be k-th column of W^{-1}. Then, since $d^{j+1} = D_k d^j$,

$$
\begin{aligned}
d^\infty &= W^{-1}FWd^0 \\
&= (b + 2c\cos(\frac{2\pi}{k}))^\infty \cdot \left(0 \middle| w_2^{-1} \middle| 0 \middle| \cdots \middle| 0 \middle| w_k^{-1} \right) W d^0 \\
&= (b + 2c\cos(\frac{2\pi}{k}))^\infty \cdot \left(w_2^{-1}(w_2 \cdot d^0) + w_k^{-1}(w_k \cdot d^0) \right).
\end{aligned}
$$

Here, clearly, imaginary part of $\left(w_2^{-1}(w_2 \cdot d^0) + w_k^{-1}(w_k \cdot d^0) \right)$ is zero. So, we consider only real part. Then, $\mathrm{Re}(w_2) = \mathrm{Re}(w_k) = \mathrm{Re}(w_2^{-1}) = \mathrm{Re}(w_k^{-1})$. So, $\mathrm{Re}\left(w_2^{-1}(w_2 \cdot d^0) + w_k^{-1}(w_k \cdot d^0) \right) = \mathrm{Re}(2 \cdot w_2^{-1}(w_2 \cdot d^0))$. $\mathrm{Re}(w_2^{-1}(w_2 \cdot d^0)) = \mathrm{Re}(w_2^{-1}w_2)d^0$. Here, matrix $\mathrm{Re}(w_2^{-1}w_2)$ is:

$$
\mathrm{Re}(w_2^{-1}w_2) = \mathrm{Re}\begin{pmatrix}
\omega^0 & \omega^1 & \omega^2 & \cdots & \omega^{(k-1)} \\
\omega^{(k-1)} & \omega^0 & \omega^1 & \cdots & \omega^{(k-2)} \\
\omega^{(k-2)} & \omega^{(k-1)} & \omega^0 & \cdots & \omega^{(k-3)} \\
\vdots & \vdots & \vdots & \ddots & \vdots \\
\omega^1 & \omega^2 & \omega^3 & \cdots & \omega^0
\end{pmatrix}.
$$

Therefore, we can see that if k is even, then d^∞ forms regular k-gon or its expansion on tangent plane at v_0^∞. If k is odd, then d^∞ forms regular k-gon. That is because $d^{\infty+1} \propto \mathrm{Re}(w_2^{-1}w_2)d^\infty$. See Fig. 36 ($k = 6$). d_i^∞ is i-th row of d^∞. The left picture is regular hexagon. The right picture is a expansion of regular k-gon which is extend by a constant factor with a direction. These d^∞ satisfy $d^{\infty+1} \propto \mathrm{Re}(w_2^{-1}w_2)d^\infty$. Therefore, triangles of Loop type subdivision are good shapes at the limit.

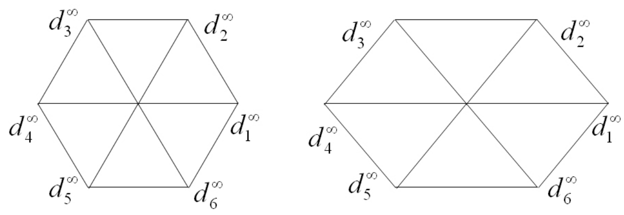

Fig. 36. Difference vectors at the limit.

5.2 Optimal schemes

Here, we consider best choices of b, c.

In previous subsection, we can see that b, c affects only eigen values. Eigen vectors are independent of b, c. Eigen values are coefficients of Laplacian and decrease of waves on concentric circles whose center is v_0^j.

First our request is that eigen values which correspond to lowest frequency part are maximal eigen values. That is, $c > 0$. Second our request is that all eigen values are non-negative. That is, $b - 2c \geq 0$. Then, components of the waves decrease monotonically. If b, c satisfy these two requests, then D_k is a low pass filter.

From our requests, $b > 0$.

Next, we consider maximization of convergence rate of the waves. That is, we maximize $\frac{b+2c\cos(\frac{2\pi}{k})}{b+2c\cos(\frac{4\pi}{k})}$. So, we maximize c.

Here, $b + c = \frac{1}{2}$. Therefore, our choice is $b = \frac{1}{3}, c = \frac{1}{6}$.

Here, we show optimal schemes. Fig. 37 is the basis function of optimal schemes with $\beta = \frac{1}{k}(\frac{2}{3} - (\frac{1}{3} + \frac{1}{3}\cos(\frac{3\pi}{k})))$ (This is high pass optimal scheme.). Here, original mesh is Fig. 23. Fig. 38 is the basis function of optimal schemes with $\beta = \frac{1}{k}(\frac{2}{3} - (\frac{1}{3} + \frac{1}{3}\cos(\frac{2\pi}{k}))^2)$. Fig. 39 is the basis function of optimal schemes with $\beta = \frac{1}{k}(\frac{33}{64})$ (This is low pass optimal scheme.). Fig. 40 is the basis function of Loop subdivision scheme.

On regular part, fairness of basis functions of optimal scheme with $\beta = \frac{1}{k}(\frac{2}{3} - (\frac{1}{3} + \frac{1}{3}\cos(\frac{2\pi}{k}))^2)$ or $\frac{1}{k}(\frac{33}{64})$ is smaller than that of basis function of Loop subdivision. In Fig. 41, the green surface is basis function of Loop subdivision. The pink surface is basis function of high pass optimal scheme. In Fig. 42, the green surface is basis function of Loop subdivision. The pink surface is optimal scheme with $\beta = \frac{1}{k}(\frac{2}{3} - (\frac{1}{3}+\frac{1}{3}\cos(\frac{2\pi}{k}))^2)$. In Fig. 43, the green surface is basis function of Loop subdivision. The pink surface is basis function of low pass optimal scheme.

In Fig. 44, the green surface is basis function of high pass optimal scheme. The

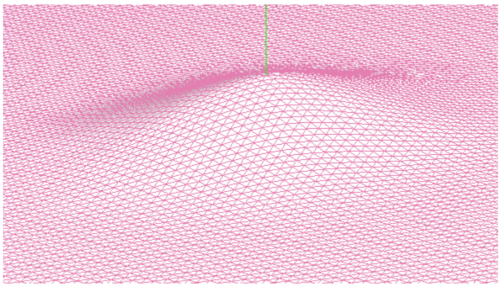

Fig. 37. Basis function of high pass optimal scheme

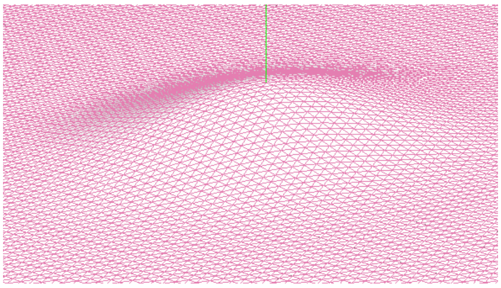

Fig. 38. Basis function of optimal scheme $\beta = \frac{1}{k}(\frac{2}{3} - (\frac{1}{3} + \frac{1}{3}\cos(\frac{2\pi}{k}))^2)$.

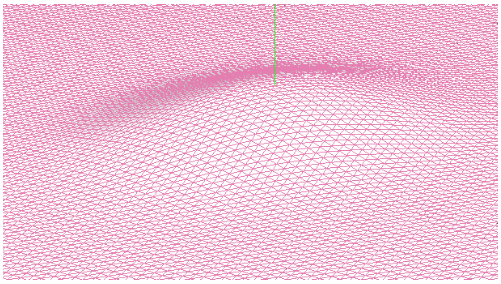

Fig. 39. Basis function of low pass optimal scheme.

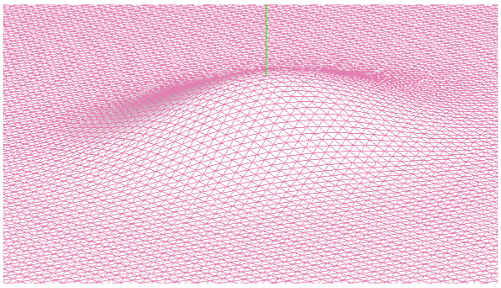

Fig. 40. Basis function of Loop subdivision.

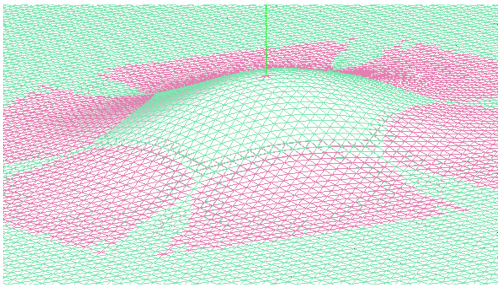

Fig. 41. Basis functions of Loop and high pass optimal.

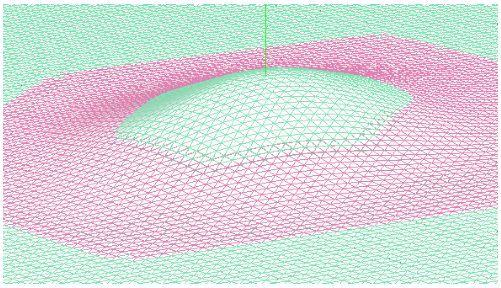

Fig. 42. Basis functions of Loop and optimal scheme $\beta = \frac{1}{k}(\frac{2}{3} - (\frac{1}{3} + \frac{1}{3}\cos(\frac{2\pi}{k}))^2)$.

pink surface is basis function of optimal scheme with $\beta = \frac{1}{k}(\frac{2}{3} - (\frac{1}{3} + \frac{1}{3}\cos(\frac{2\pi}{k}))^2)$. In Fig. 45, the green surface is basis function of optimal scheme with $\beta = \frac{1}{k}(\frac{2}{3} - (\frac{1}{3} + \frac{1}{3}\cos(\frac{2\pi}{k}))^2)$. The pink surface is basis function of low pass optimal scheme.

Moreover, in Fig. 46, the green surface is optimal subdivision surface with $\beta = \frac{1}{k}(\frac{2}{3} - (\frac{1}{3} + \frac{1}{3}\cos(\frac{2\pi}{k}))^2)$. The pink surface is low pass optimal subdivision surface. Here, original mesh is the cube in Fig. 29. So, we can see that if $k \geq 5$, then fairness of $\beta = \frac{1}{k}(\frac{33}{64})$ is smaller than that of $\beta = \frac{1}{k}(\frac{2}{3} - (\frac{1}{3} + \frac{1}{3}\cos(\frac{2\pi}{k}))^2)$.

Therefore, optimal schemes generate good subdivision surfaces. On regular part, fairness of some optimal schemes is smaller than that of Loop subdivision.

Note that above optimal schemes are C^1-continuous. Using the analysis in [2], we can get the necessary and sufficient condition for optimal schemes to be C^1-

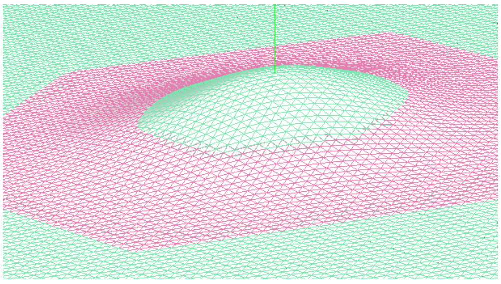

Fig. 43. Basis functions of Loop and low pass optimal.

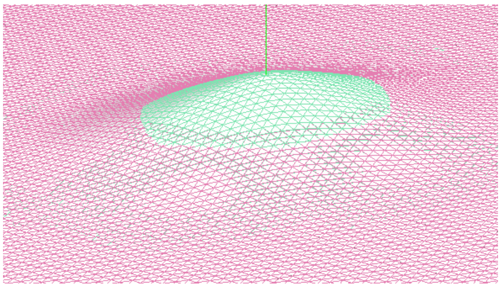

Fig. 44. Basis functions of high pass optimal and optimal with $\beta = \frac{1}{k}(\frac{2}{3} - (\frac{1}{3} + \frac{1}{3}\cos(\frac{2\pi}{k}))^2)$.

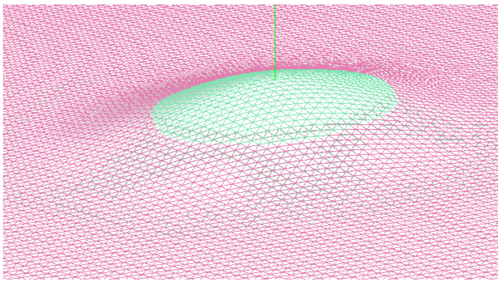

Fig. 45. Basis functions of $\beta = \frac{1}{k}(\frac{2}{3} - (\frac{1}{3} + \frac{1}{3}\cos(\frac{2\pi}{k}))^2)$ and low pass optimal.

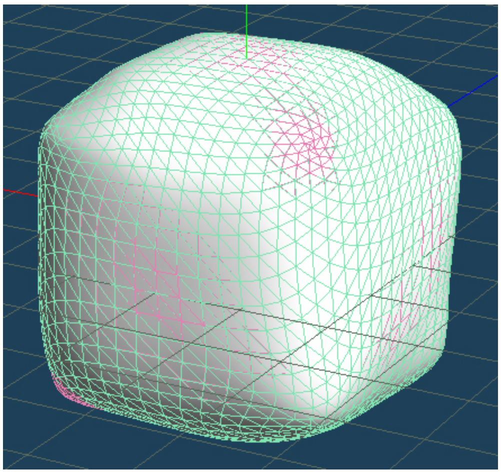

Fig. 46. Optimal subdivision surface with $\beta = \frac{1}{k}(\frac{2}{3} - (\frac{1}{3} + \frac{1}{3}\cos(\frac{2\pi}{k}))^2)$ and low pass optimal subdivision surface.

continuous. In fact, optimal subdivision scheme is C^1-continuous if and only if $|b + 2c - k\beta| < |b + 2c\cos(\frac{2\pi}{k})|$ (Here, $b = \frac{1}{3}, c = \frac{1}{6}$.).

6 Conclusion

In this paper, we proposed “Laplacian subdivision” and “optimal scheme”.

Laplacian subdivision use a new subdivision matrix which is linear combination fo ordinary subdivision matrix and Laplacian operator. Then, we could define high pass Laplacian subdivision and low pass Laplacian subdivision. In this paper, we defined Laplacian Loop subdivision. Moreover, we derived the necessary and sufficient condition of C^1-continuity of Laplacian Loop subdivision. So, we could generate C^1 Laplacian Loop subdivision surfaces.

Next, we defined Laplacian butterfly subdivision. Laplacian butterfly subdivision is an interpolate subdivision. Similarly, we could define high pass Laplacian butterfly subdivision and low pass Laplacian butterfly subdivision by stencils. On regular part, we checked C^1-continuity of some low pass Laplacian butterfly subdivision.

Finally, we analyze Loop type subdivision. Then, we could understand effects of all elements of stencils. A eigen value of D_k corresponds to Laplacian. Other eigen values of D_k affect waves on concentric circles whose center is v_0^j. Eigen value of Laplacian of D_k affects a wave which is vertically on other waves.

Thus, we choiced elements of stencils such that high frequency part of the waves on the concentric circles are decreased fastest. Then, we defined "optimal scheme" as subdivision schemes which have this choice of elements of stencil. Optimal schemes generate good subdivision surfaces. On regular part, fairness of some optimal schemes is smaller than that of Loop subdivision.

Acknowledgments

This work is supported by the 21st Century COE Program on Information Science Strategic Core of the Ministry of Education, Science, Sports and Culture of Japan.

References

[1] H. Kawaharada, K. Sugihara, c^k-continuity of stationary subdivision schemes, METR 2006-01, The University of Tokyo (January 2006).

[2] H. Kawaharada, K. Sugihara, c^k-continuity of stationary subdivisions, Computer Aided Geometric Design XX (2006) submitted.

[3] C. T. Loop, Smooth subdivision surfaces based on triangles, Master's thesis, University of Utah, Department of Mathematics (1987).

[4] J. Warren, H. Weimer, Subdivision Methods for Geometric Design: A Constructive Approach, Morgan Kaufmann Publishers, 1995.

[5] D. Zorin, Smoothness of stationary subdivision on irregular meshes, Constructive Approximation 16 (3) (2000) 359–397.

[6] U. Reif, A unified approach to subdivision algorithms near extraordinary points, Computer Aided Geometric Design 12 (1995) 153–174.

[7] H. Prautzsch, Analysis of c^k-subdivision surfaces at extraordinary points, Preprint. Presented at Oberwolfach.

[8] A. S. Cavaretta, W. Dahmen, C. A. Micchell, Stationary subdivision, Memoirs Amer. Math. Soc. 93(453).

[9] T. N. T. Goodman, C. A. Micchell, W. J. D., Spectral radius formulas for subdivision operators, in: L. L. Schumaker and G. Webb, editors, Recent Advances in Wavelet Analysis, Academic Press, 1994, pp. 335–360.

[10] D. Zorin, Subdivision and multiresolution surface representations, Ph.D. thesis, University of California Institute of Technology (1997).

[11] U. Reif, A degree estimate for polynomial subdivision surfaces of higher regularity, Proc. Amer. Math. Soc. 124:2167–2174.

[12] D. Doo, M. A. Sabin, Behaviour of recursive subdivision surfaces near extraordinary points, Computer Aided Geometric Design 10 (1978) 356–360.

[13] G. Taubin, A signal processing approach to fair surface design, in: SIGGRAPH 95 Conference Proceedings, ACM, 1995, pp. 351–358.

[14] D. Zorin, P. Schroder, W. Sweldens, Interpolating subdivision for meshes with arbitrary topology, in: SIGGRAPH 96 Conference Proceedings, ACM, 1996, pp. 189–192.

[15] E. J. Stollnitz, T. D. DeRose, D. H. Salesin, Wavelets for Computer Graphics: Theory and Applications, Morgan Kaufmann Publishers, 1996.

[16] H. Kawaharada, K. Sugihara, Computation of normals for stationary subdivision surfaces, in: the fourth International Conference on Geometric Modeling and Processing, Pittsburgh, 2006.